On the Sensitivity Analysis in Reliability Evaluation for Power Electronic Converters

Yubo Song, *Member, IEEE*, Pascal A. Schirmer, Peter Schreivogel, Kaichen Zhang, *Member, IEEE*, Huai Wang, *Senior Member, IEEE*, and Frede Blaabjerg, *Fellow, IEEE*

***Abstract*—Power electronic converters are essential in modern electrical and electronic applications, necessitating the study on power electronic reliability for dependable design and operation. In earlier research on power electronic reliability, the mission profiles have been mapped to thermal stresses and lifetimes, while its applications are generally focused on steady-state scenarios. It turns out to be time-consuming and inefficient to repeat the entire procedures for addressing the impact of stress variances or model uncertainties. In this context, this article defines the sensitivity for power electronic reliability and provides a sensitivity-based perspective on system optimization, where the concept is formulated through two steps, accounting for thermal stresses and lifetime, respectively. The applications of sensitivities for thermal stresses and lifetime are demonstrated, which serve as identifiers of critical factors and quantitative metrics of marginal performances. Upon this, possibilities are also emerging for enhancing the cost-effectiveness of reliability validations and encompassing model robustness into reliability analysis and prediction.**

***Index Terms*—Converters, lifetime, power electronics, reliability, sensitivity analysis, thermal stresses.**

I. Introduction

POWER electronic converters have become the core interfaces of diverse electrical and electronic applications [1], [2], where power semiconductors play critical roles. With energy conversion being one of the primary functional requirements, the efficiency and power density of power electronic converters have been improved with cutting-edge components, topologies, and operation strategies [3], [4], [5]. Meanwhile, acknowledged as a critical performance metric, reliability has emerged to be another key dimension of performances of power electronic applications during long-term field operation [6], which can be leveraged to reduce the overall economic costs including maintenance. In this context, the *lifetime* of components and systems, stemming from conventional reliability engineering, has become one of the critical metrics.

Received 12 September 2024; revised 16 December 2024; accepted 5 January 2025. Date of publication 15 January 2025; date of current version 26 February 2025. Recommended for publication by Associate Editor K. Ma. *(Corresponding authors: Yubo Song; Pascal A. Schirmer.)*

Yubo Song, Kaichen Zhang, Huai Wang, and Frede Blaabjerg are with the Department of Energy (AAU Energy), Aalborg University, DK-9220 Aalborg, Denmark (e-mail: yuboso@energy.aau.dk; kzh@energy.aau.dk; hwa@energy.aau.dk; fbl@energy.aau.dk).

Pascal A. Schirmer and Peter Schreivogel are with the BMW Group Research and Innovation Center, 80788 Munich, Germany (e-mail: pascal.schirmer@bmw.de; peter.schreivogel@bmw.de).

Color versions of one or more figures in this article are available at https://doi.org/10.1109/TPEL.2025.3530148.

Digital Object Identifier 10.1109/TPEL.2025.3530148

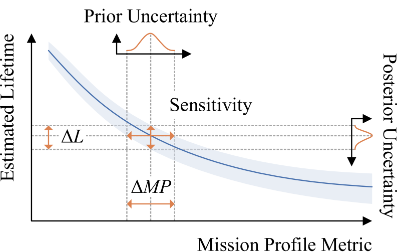

Fig. 1. Forming sensitivity analysis for power electronic reliability. Sensitivity serves as an effective metric mapping the prior uncertainty of mission profiles (ΔMP) into posterior uncertainty of lifetime (ΔL).

The large variation of power electronic components has made it challenging to develop empirical models comprehensively embracing all types of components. Going beyond the experience-driven methodologies described by failure rate [7], reliability analysis through component *failure mechanisms* [or physics-of-failure (PoF)] is suggested [8], which navigates the lab tests and can handily adapt the reliability models to varied mission profiles.

One of the typical types of failures of power electronic converters, wear-out failures, is dependent on the degradation of components [9]. Power semiconductors and capacitors are generally among the major components prone to wear-out failures [10], and the operational stresses influence how fast components will degrade. Thermal stresses, for instance, can typically be influenced by the converter topology and thermal interactions, but compromise among the components is often inevitable. To best distribute the stresses and achieve longer lifetime at the system level, it is thus worthwhile to optimize the design and operation of converters based on reliability models and/or metrics, namely, the reliability-oriented design [11], [12], [13] and control [14], [15], [16].

Previous literature, such as [17], has enlightened a widely used framework of mission profile-based reliability analysis for power electronic converters. The lifetimes of components and the entire system are evaluated by analyzing the thermal stresses, which originate from mission profiles as per the PoF. However, when considering the influences of small-signal perturbations/uncertainties, such as errors or drifts of the parameters or mission profiles, it can be time-consuming to repeat the process of thermal evaluation, which normally concerns

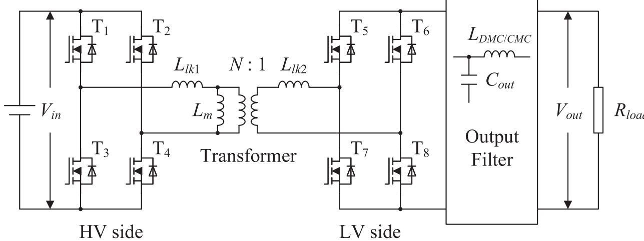

Fig. 2. DAB converter studied in this article, which is divided into HV side and LV side.

TABLE I
RATED PARAMETERS OF THE STUDIED SYSTEM

Parameters	Value
Input voltage V_{in}	200 V
Output voltage V_{out}	13.5 V
Switching frequency f_{sw}	100 kHz
Loading power P_{load}	1800 W
Trafo. transformation ratio N:1	10:1
Trafo. leakage inductance $L_{\mathrm{lk1,2}}$	1 μH, 0.02 μH
Output filter capacitance C_{out}	5.5 μF
Ambient temperature T_{amb}	35°C
Power rating of HV devices	750 V, 20 A
Power rating of LV devices	100 V, 300 A

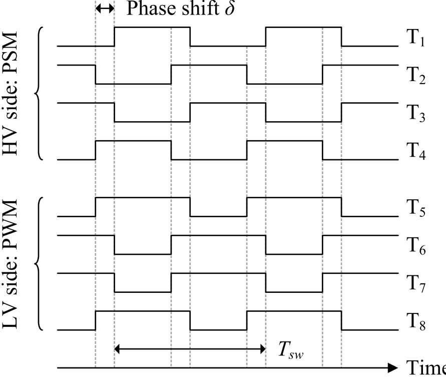

Fig. 3. Illustration of the drive signals for the modulation method adopted in this article for the studied DAB converter in Fig. 2.

slow dynamics and long timescales. In addition, quantification of small-signal perturbations/uncertainties is also the key to enhance the robustness of reliability modeling, which has not yet been well explored either.

Inspired by the sensitivity analysis of power systems [18], this article thereby aims to unravel this aspect in power electronic reliability optimization, formulating *sensitivity* likewise for power electronic reliability that can serve as an instructive metric indicating the role of small-signal perturbations/uncertainties, as illustrated in Fig. 1. In general, prior variation or uncertainty of mission profiles (ΔMP) introduces posterior variation or uncertainty of lifetime (ΔL) as per the physics, and the changing rate formulates the said *sensitivity*, quantifying system performances under disturbances. Different from the probabilistic sensitivity for reliability engineering in [19], this article emphasizes the role of PoF in power electronic applications and defines sensitivity in two steps as aligned with the reliability evaluation for power electronics, concerning the thermal stresses and estimated lifetime. By demonstrating their applications with case studies, the significance is highlighted in providing guidelines for operational sensing and optimizing the design of power electronic converters.

The rest of this article is organized as follows. Section II elaborates on the reliability model of power electronic components adopted. Sections III and IV introduce the concepts of sensitivity in reliability analysis for thermal stresses and lifetime, respectively, and how it can be leveraged in power electronic applications, through demonstrations on industrial case studies. Section V extends on discussions from the perspective of industrial testing and manufacturing. Finally, Section VI concludes this article with future visions on this topic.

II. Thermal Stresses and Reliability Modeling of Power Electronic Converters

The reliability of power electronic converters is normally evaluated based on the PoF of power electronic components [8] highlighting the roles of mission profiles and thermal stresses, which is employed in this article. To manifest this, a dual-active-bridge (DAB) dc–dc converter is selected as the study case, of which the topology is illustrated in Fig. 2, and key parameters of the case illustrated in Fig. 2 are specified in Table I unless otherwise specified. The high-voltage (HV) and low-voltage (LV) sides operate in phase-shift modulation and pulsewidth modulation, respectively, and exemplary drive signals are accordingly depicted in Fig. 3.

The power semiconductors (SiC MOSFETs from Infineon with preliminary datasheets) in the study case are preliminarily identified as the most critical and fragile components. Without loss of generality, other components, such as capacitors, are assumed to be sufficiently reliable throughout the analysis, considering that they operate under approximately constant mission profiles, and they are relatively less sensitive to the studied mission profiles.

The widely used lifetime models of power semiconductors (both IGBT [20] and SiC [21]) are deduced from power cycling tests. The models combine the Coffin–Manson law and the Arrhenius law [22], which can be expressed as (1). The cycles of junction temperature (power cycles, as shown in Fig. 4) lead to the mechanical stresses, which accumulate over time, and the lifetime, in number of cycles, is principally influenced by the junction temperature T_{j} (mean value $T_{\mathrm{j,m}}$ or minimum value $T_{\mathrm{j,min}}$ over the power cycles) and the magnitude of its swing ΔT_{j} in the power cycles, as well as other key factors, including ON-state time (or temperature-rising time) t_{on}, bondwire current I_{bw}, voltage level V, and bondwire diameter D, as in

$$N_f = N_0 \cdot \Delta T_{\mathrm{j}}^{\beta_1} \cdot \exp\left(\frac{\beta_2}{T_{\mathrm{j}}}\right) \cdot t_{\mathrm{on}}^{\beta_3} \cdot I_{\mathrm{bw}}^{\beta_4} \cdot V^{\beta_5} \cdot D^{\beta_6} \quad (1)$$

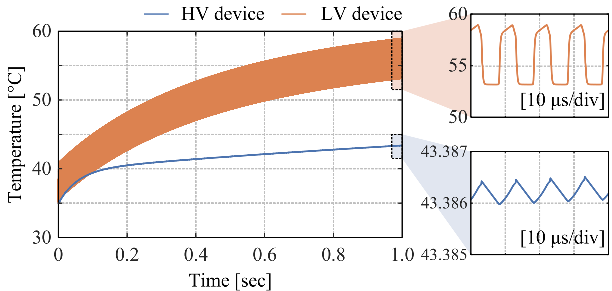

Fig. 4. Example of junction temperatures rising over time, where both the mean junction temperature and temperature swing have impacts on the lifetime of devices.

where T_j is in Kelvin (K), N_f is the estimated lifetime in number of cycles, and N_0, β_1, β_2, β_3, β_4, β_5, and β_6 are the coefficients obtained from experimental tests.

Remark 1: It should be noted that the model specified by (1) only involves the most primary failure mechanisms for power semiconductors, and all the factors are assumed not to deviate significantly from the rated conditions. Encompassing more factors may impel additional terms in the product, and irregular factors may need to be described by specialized lifetime models.

In this article, it is assumed that the change of ON-state time t_on has negligible influence, and the bondwire current I_bw, voltage level V, and bondwire diameter D do not change by cases. Thus, the corresponding terms can be absorbed into N_0 as a more inclusive coefficient N_0', namely

$$N_f = N_0' \cdot \Delta T_\mathrm{j}^{\beta_1} \cdot \exp\left(\frac{\beta_2}{T_\mathrm{j}}\right). \tag{2}$$

The power cycles can thereby be classified based on the mission profiles $\{T_\mathrm{j}, \Delta T_\mathrm{j}\}$.

Remark 2: The power cycles are identical and evenly distributed over time in the case depicted in Fig. 4, the number of which is therefore proportional to time periods. In more general cases, the power cycles aroused by time-variant loading profiles should be analyzed in groups via *rain-flow counting*.

Remark 3: It should be noted here that the lifetime in the model formulated by (1) and (2) stands for the B_x lifetime (an estimation of the worn-out testing samples reaches $x\%$ of the entire population), where x is specified by the application of interest and reflected in the coefficients extracted from the testing results. In this article, it is assumed that the device samples also follow the model coefficients in [20] and [21], yielding B_{10} lifetime.

To efficiently calculate $\{T_\mathrm{j}, \Delta T_\mathrm{j}\}$ for a semiconductor stack-up, as illustrated in Fig. 5(a), model order reduction techniques can be used [23]. In the present study, thermal relations are modeled based on electrical series network representations also called Foster models [24]. In detail, both the thermal path from the junction of a semiconductor and the thermal path from the semiconductor case to the ambient are modeled.

In Fig. 5(b), a Foster network with K layers is shown, including a thermal resistance (R_th^k) and a thermal capacitance (C_th^k) for each layer, a loss source (P_loss), and a reference temperature (T_amb), e.g., the ambient or coolant temperature. The transient

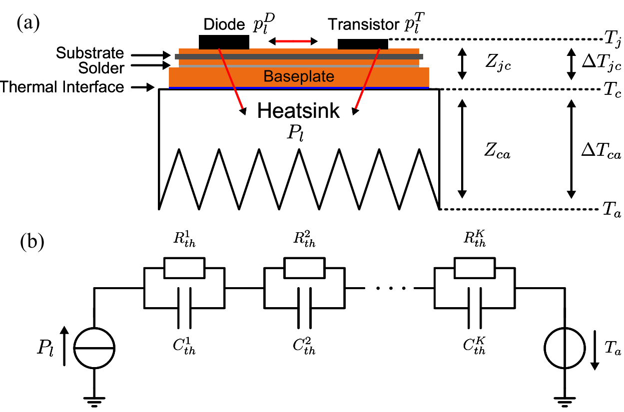

Fig. 5. (a) Thermal semiconductor stack-up, including chips, substrate, solder, and baseplate, as well as (b) reduced order thermal network using Foster network representation.

thermal impedance can then be modeled as in the following equation using a set of K exponential functions:

$$Z_\mathrm{th} = \sum_{k=1}^{K} R_\mathrm{th}^k \left(1 - e^{-t/\tau_k}\right) \tag{3}$$

where $Z_\mathrm{th}(t)$ is the total transient thermal impedance and $\tau_k = R_\mathrm{th}^k C_\mathrm{th}^k$ is the time constant of the kth layer. Consequently, T_j can be calculated as

$$T_\mathrm{j} = T_\mathrm{amb} + \Delta T_\mathrm{j} = T_\mathrm{amb} + P_\mathrm{loss} * (Z_\mathrm{ca} + Z_\mathrm{jc}) \tag{4}$$

where "*" denotes the convolution of the transient thermal impedance $Z_\mathrm{ca/jc}$ with the power losses P_loss. It should be noted that it is assumed that $Z_\mathrm{th} = Z_\mathrm{ca} + Z_\mathrm{jc}$ already includes the coupling of transistor ($p_\mathrm{loss}^\mathrm{T}$) and diode losses ($p_\mathrm{loss}^\mathrm{D}$).

Based on the thermal stress caused by $\{T_\mathrm{j}, \Delta T_\mathrm{j}\}$, the lifetime can be translated into number of cycles to failure using (1) or (2) and subsequently into the time-to-failure by Miner's rule [25]. As expressed in (5), the operational damage or lifetime consumption of a power semiconductor, if normalized, accumulates by the number of endured power cycles from the beginning

$$D = \sum_i \frac{n^{(i)}}{N_f^{(i)}} \tag{5}$$

where $n^{(i)}$ and $N_f^{(i)}$ denote the counted number of the power cycles and corresponding cycles-to-failure, respectively, in the ith time period, given that the studied time period is sufficiently short compared with the entire lifetime and the damage accumulation can be linearly approximated [25]. If multiple types of power cycles are involved, the normalized accumulated damage of a specific type of power cycles would be calculated as the number of the cycles $n^{(i,j)}$ divided by the corresponding cycles-to-failure $N_f^{(i,j)}$, which indicates the consumed proportion of total availability, and then, a sum is taken for all the individual damages as a linear combination indicating the overall damage accumulation.

By the end-of-life of the device, the normalized damage D should be approximately accumulated to 1 (or 100% of the

usable lifetime despite the types of mission profiles), thus D can be mapped into the B_x lifetime by considering the time length of the power cycles.

Moreover, the reliability of power devices can also be described as a probability of reliable operation, which is needed for the system-level reliability evaluation for power electronic converters. The time-to-failure data generally follow the Weibull distribution as:

$$R(t) = \exp\left[-\left(\frac{t}{\eta}\right)^{\beta}\right] \tag{6}$$

where β and η are the shaping factor and the characteristic lifetime of the distribution, respectively. The aforementioned B_x lifetime corresponds to the time instant t when the accumulated probability of failure $F(t)$ equals $x\%$, or the reliability $R(t)$ equals $1 - x\%$.

If no redundant components are considered, then the system-level reliability of a power electronic converter requires all components to be reliable, which is

$$R_{\text{sys}}(t) = \prod_{j} R_{\text{device}}^{(j)}(t). \tag{7}$$

By solving the equation $R_{\text{sys}}(t) = 1 - x\%$, the B_x lifetime of the converter can be obtained, as the expected lifetime.

III. Sensitivity Analysis on Thermal Stresses

The reliability of power electronic converters and systems is influenced by various factors in relation to mission profiles and system configurations, while the factors normally participate to distinct extents. To this end, the sensitivity in power electronic reliability analysis for typical scenarios is worthwhile to be defined. Generally, reliability analysis for power electronic converters and systems can be divided into two steps, the mapping from mission profiles to the stresses and from stresses to the lifetime. As it is not straightforward to map the mission profile metrics directly to lifetime, the sensitivity analysis will likewise be formulated based on the two steps and connected thereafter, which will be discussed in the following sections individually alongside demonstrations on industrial case studies.

A. Formulating Sensitivity for Thermal Stresses

To facilitate the analysis, an exemplary scenario of the study case is first presented in Fig. 6. The thermal stresses, or more specifically, junction temperature T_{j} and its swing ΔT_{j} as per Section II, are influenced by the loading power P_{load} and the ambient temperature T_{amb}, while the rate of change may vary for different stress metrics or different devices.

It is reasonable to assume the relationships from mission profiles to thermal stresses to be continuous and differentiable. To describe this, the sensitivity matrix of thermal stresses can be defined as

$$\mathbf{J}_{\text{T}} = \begin{bmatrix} \frac{\partial T_{\text{j}}}{\partial P_{\text{load}}} & \frac{\partial T_{\text{j}}}{\partial T_{\text{amb}}} \\ \frac{\partial \Delta T_{\text{j}}}{\partial P_{\text{load}}} & \frac{\partial \Delta T_{\text{j}}}{\partial T_{\text{amb}}} \end{bmatrix}. \tag{8}$$

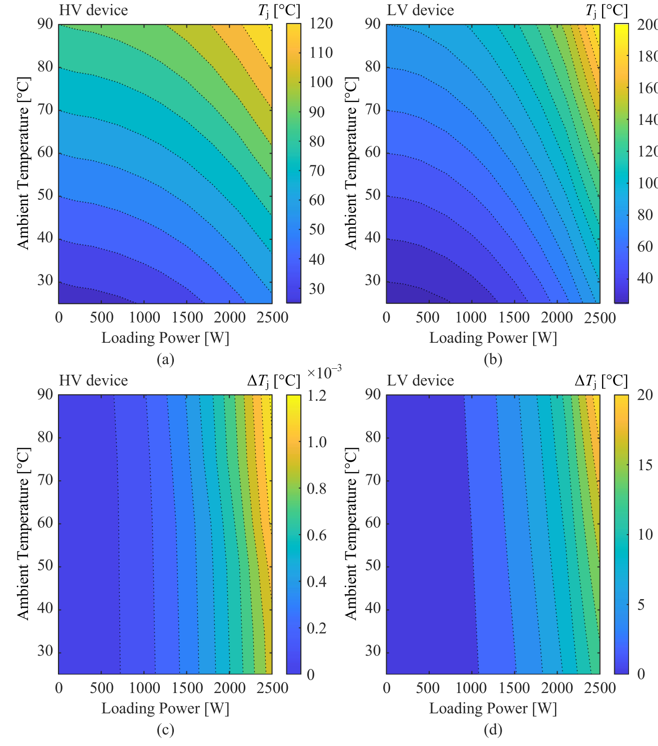

Fig. 6. Contour plot of the thermal stress metrics T_{j} and ΔT_{j} subject to the mission profile metrics T_{amb} and P_{load} for HV and LV switches: (a) and (b) mean junction temperatures T_{j}, and (c) and (d) junction temperature swings ΔT_{j} in the power cycles.

Or more generally, the sensitivity analysis can be extended to other system configuration or mission profile metrics, as

$$\mathbf{J}_{\text{T}}(\boldsymbol{\xi}) = \nabla_{\boldsymbol{\xi}} \mathbf{T} \tag{9}$$

where $\mathbf{T}$ stands for the vector for thermal stresses and $\boldsymbol{\xi}$ for studied mission profile metrics. It is numerically equivalent to the Jacobian matrix between the stresses and mission profiles.

An example is given based on (8), where the sensitivity matrix of the study case is calculated and depicted in Fig. 7. The sensitivities of HV and LV devices do not exhibit identical trends as a result of different loss models, and the monotonicity can be dependent on whether conduction or switching loss plays a more dominant role. In general, the following points can be inferred.

1) The precision required for sensing and control for testing or operation under condition monitoring. For example, if a $\pm 10\%$ variation of the loading power P_{load} is studied around the rated value 1800 W, then the junction temperature T_{j} of HV device will change by around 3.1°C, which should be able to be detected and distinguished by the employed thermal sensors.
2) If the stresses are sensitive to mission profiles, then in case of, e.g., active thermal control of power electronic converters, higher robustness should be underlined concerning mission profile uncertainty.

Furthermore, the analytical expressions of the mapping relationships from mission profiles to the thermal stresses can be complicated and inconsistent for different scenarios. Consequently, a convenient approach is to quantify the relationships

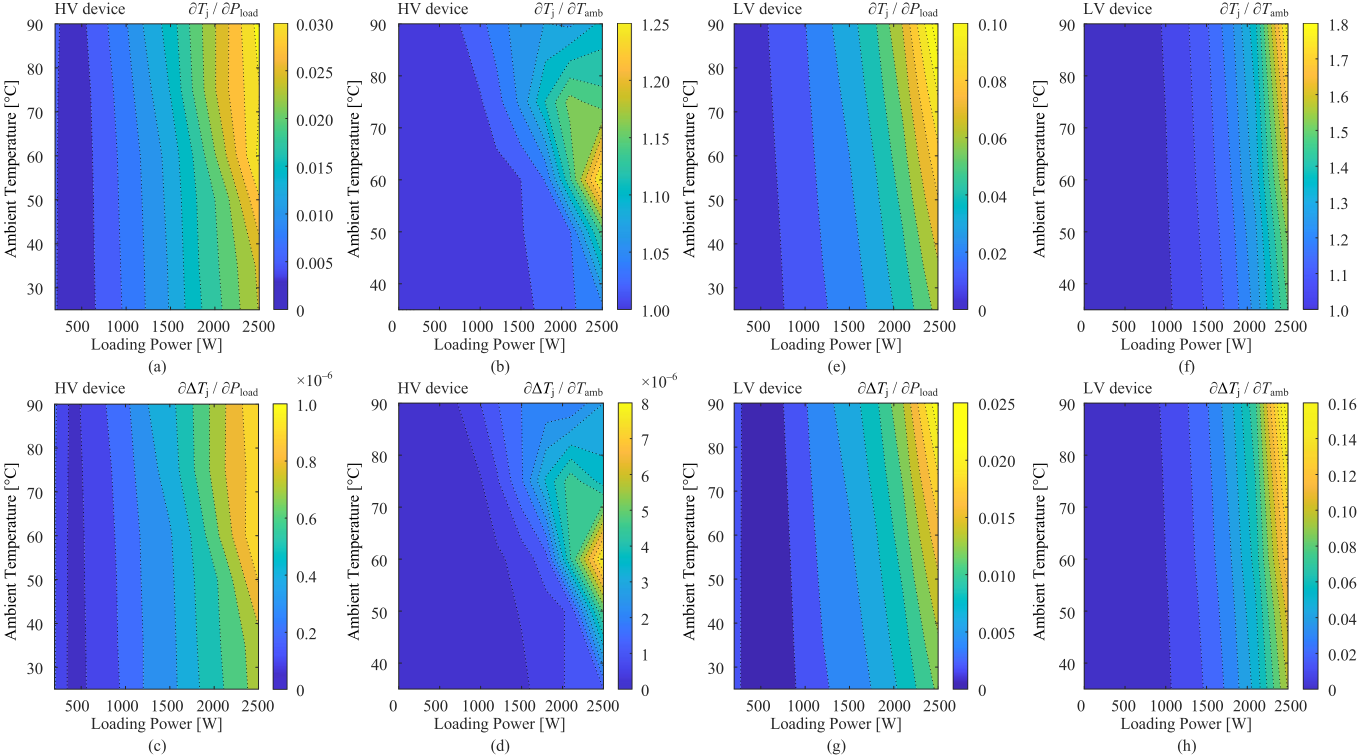

Fig. 7. Thermal stress sensitivity of the studied devices subject to the mission profile metrics T_{amb} and P_{load}: (a)–(d) for HV device, and (e)–(h) for LV device. The sensitivity metrics are labeled to the top of each subfigure individually.

into numerical fittings (e.g., polynomial expressions) based on the data from simulations or tests at a number of operation points, such as

$$\hat{T}_{\text{j}} = f_1\left(P_{\text{load}}, T_{\text{amb}}\right)$$
$$\hat{T}_{\text{jsw}} = f_2\left(P_{\text{load}}, T_{\text{amb}}\right) \tag{10}$$

where $f_1(\cdot)$ and $f_2(\cdot)$ are derived polynomial fitting functions. Then, the sensitivity matrix can alternatively be expressed into

$$\mathbf{J}_{\text{T}} \approx \begin{bmatrix} \frac{\partial f_1}{\partial P_{\text{load}}} & \frac{\partial f_1}{\partial T_{\text{amb}}} \\ \frac{\partial f_2}{\partial P_{\text{load}}} & \frac{\partial f_2}{\partial T_{\text{amb}}} \end{bmatrix}. \tag{11}$$

The thermal stresses can then be estimated based on the following equation as per the Taylor's Theorem:

$$\Delta \begin{bmatrix} T_{\text{j}} \\ \Delta T_{\text{j}} \end{bmatrix} = \mathbf{J}_{\text{T}} \Delta \begin{bmatrix} P_{\text{load}} \\ T_{\text{amb}} \end{bmatrix} + o\left(\left\| \Delta \begin{bmatrix} P_{\text{load}} \\ T_{\text{amb}} \end{bmatrix} \right\|\right) \tag{12}$$

where $o(\cdot)$ denotes higher order infinitesimal terms. In a more general form, (12) can be expressed as

$$\Delta \mathbf{T} = \mathbf{J}_{\text{T}}(\boldsymbol{\xi})\Delta\boldsymbol{\xi} + o\left(\|\Delta\boldsymbol{\xi}\|\right) \approx \mathbf{J}_{\text{T}}\Delta\boldsymbol{\xi}. \tag{13}$$

The small-signal influences of mission profile uncertainties can thus be quantified.

From this perspective, sensitivity analysis can be employed to account for mission profile uncertainties in reliability modeling, thereby laying the basis for robust reliability-oriented control for power electronic converters and systems.

B. Extensions With Experimental Testing Results

To further manifest the applications of sensitivity analysis, an industrial DAB converter system from BMW is thereby studied and tested by validating the stress differences among the devices in the same system during regular operations. The layout of the study case is illustrated in Fig. 8. In details, Fig. 8 includes the chip placement in the x–y plane, the layer stack-up in the z-direction, and the measured as well as calculated transient thermal impedance curves. Two channels are placed in each circuit board, and the system is divided into HV and LV boards. Temperatures are measured by thermocouples touching the surface of power devices, which however should be the case temperatures T_{c} but are generally in positive correlation with the junction temperatures or thermal stresses. The measurements are identified as labeled in Fig. 8.

A group of the measurement results is presented in Fig. 9. The temperatures rise over time, meanwhile the differences are shown among the components, due to the inconsistencies in component parameters and spacial positioning in practice. Following this point, experimental tests are conducted where the coolant temperature is varied, with the results given in Table II.

It is noticed that in this case, the measured case temperatures approximately increase linearly upon the coolant temperature. Hence, the sensitivity $\partial T_{\text{c}}/\partial T_{\text{amb}}$ is calculated as the slope of the linear fitting of the relationship, which is also given in Table II. This sensitivity is physically determined by the thermal networks between the devices and the ambient, and helps to identify the

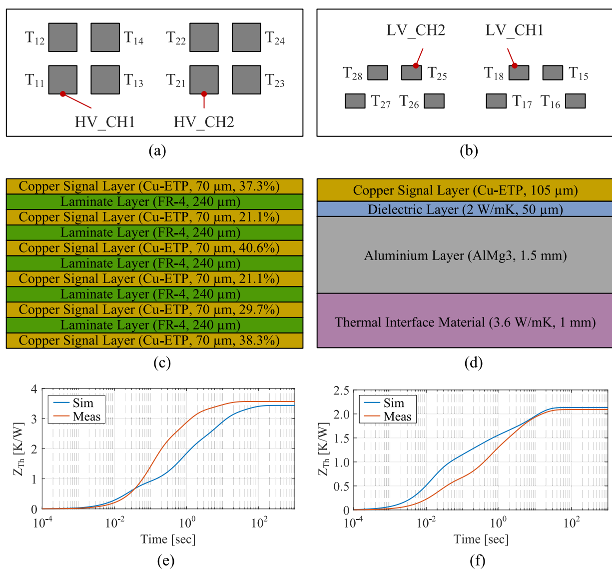

Fig. 8. Illustration of the layout of the DAB system under test, including the chip placement in (a) and (b), the layer stack-up of the PCBs in (c) and (d), and the measured [*Meas.* in the legends of (d) and (f)] as well as simulated [*Sim.* in the legends of (d) and (f)] transient thermal impedance curves for HV (left) and LV boards (right), respectively. (a) HV chips PCB placement. (b) LV chips PCB placement. (c) HV PCB layer stack-up. (d) LV PCB layer stack-up. (e) HV chips thermal impedance. (f) LV chips thermal impedance.

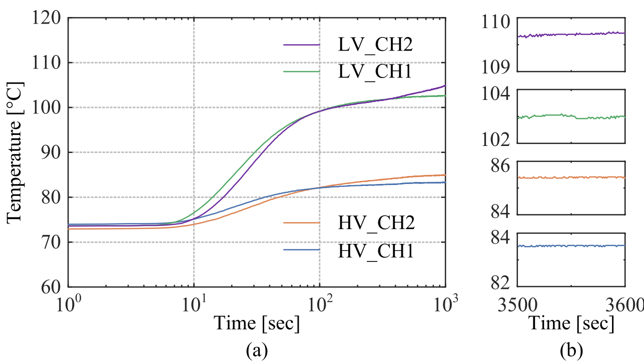

Fig. 9. Exemplary temperature rise data measured by thermocouples during the test where $T_{\mathrm{amb}} = 75°$C, including: (a) heating-up process and (b) steady-state temperature.

sources of stresses on the devices. For example, by comparing HV devices, CH1 (T_{11}) is 5.7% more sensitive to the change of ambient temperature due to the spacial design in relation to the heat dissipation as well as thermal coupling with other components, while CH2 (T_{21}) ends up with suffering from higher stress, which should be recognized as a consequence of self-heating.

IV. Sensitivity Analysis on Lifetime

A. Sensitivity From the Lifetime Model

Similar to Section III, the sensitivity for the lifetime can be formulated, which is more transparent with the lifetime model in Section II from the thermal stresses. By taking the partial derivatives of N_f in (1) or (2), the sensitivity for the lifetime (in

TABLE II
Device Temperature Measurements and Sensitivity Analysis With Experimental Tests

Measured Devices	Coolant Temperature					$\frac{\partial T_c}{\partial T_{\mathrm{amb}}}$
	35°C	45°C	55°C	65°C	75°C	
HV_CH1	46.3	55.9	65.3	74.3	83.5	0.93
HV_CH2	50.0	59.0	67.9	76.4	85.4	0.88
LV_CH1	71.8	80.2	88.1	95.2	103.0	0.77
LV_CH2	78.1	87.0	99.6	103.9	110.7	0.82

Note: All temperature data in °C.

number of cycles) can be defined as follows:

$$S_{N_f}(\Delta T_{\mathrm{j}}) = \frac{\partial N_f}{\partial \Delta T_{\mathrm{j}}} = N_f \cdot \left(\beta_1 \Delta T_{\mathrm{j}}^{-1}\right) \tag{14a}$$

$$S_{N_f}(T_{\mathrm{j}}) = \frac{\partial N_f}{\partial T_{\mathrm{j}}} = N_f \cdot \left(-\beta_2 T_{\mathrm{j}}^{-2}\right). \tag{14b}$$

In this way, the change of device lifetime is quantified upon small-signal variances of stresses, which is determined by the type of device. By extracting N_f from (14), the sensitivity can be expressed into the normalized form as

$$S^{(\mathrm{n})}_{N_f}(\Delta T_{\mathrm{j}}) = \frac{\partial N_f / N_f}{\partial \Delta T_{\mathrm{j}} / \Delta T_{\mathrm{j}}} = \beta_1 \tag{15a}$$

$$S^{(\mathrm{n})}_{N_f}(T_{\mathrm{j}}) = \frac{\partial N_f / N_f}{\partial T_{\mathrm{j}}} = -\beta_2 T_{\mathrm{j}}^{-2} \tag{15b}$$

where (15a) and (15b) are the normalized sensitivity subject to per-unit change of ΔT_{j} and per-degree change of T_{j}, respectively. In the context of (15), the exact value of N_f is not a must in the sensitivity analysis.

Remark 4: The sensitivities (14) and (15) in this section are formulated for power semiconductors based on their lifetime models. For other components, such as capacitors (e.g., [26]), the formula may not be in an identical form, which stems from the Coffin–Manson law or Arrhenius law, whereas the basic idea and the framework should hold for different lifetime models.

The sensitivity analysis on T_{j} and ΔT_{j} can then be decoupled from each other after normalization. Besides, the two equations can be interpreted as the following, through an exemplary case where the coefficients are specified as $\beta_1 = -3.775$ and $\beta_2 = 1285$ [20], [21], without loss of generality.

1) From (15a), every 1% larger temperature swing ΔT_{j} induces $|\beta_1|$% shorter estimated lifetime, where $\beta_1 < 0$ (3.78% decrease in the example).
2) With (15b), the normalized lifetime sensitivity of the study case can be deduced as plotted in Fig. 10. For example, around the operation point of $T_{\mathrm{j}} = 60°$C, every 1°C decrease of junction temperature T_{j} corresponds to an estimation of 1.15% longer lifetime.

B. Evaluations on the Total Sensitivity

Subsequently, the sensitivity from mission profiles to the lifetime is formulated by connecting the two steps. Considering the entire procedures of reliability evaluation, the sensitivity of lifetime in relation to mission profiles can be defined according

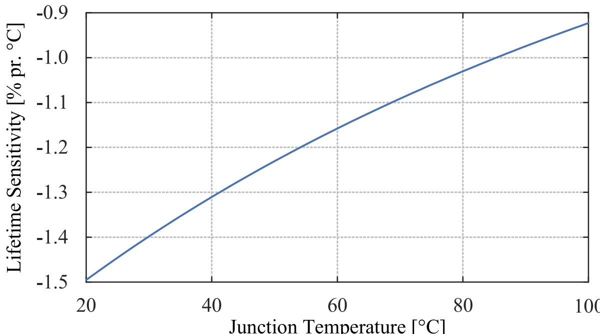

Fig. 10. Normalized sensitivity of lifetime subject to junction temperature.

to the chain rule, which is exemplified as the following if assuming that only T_j and ΔT_j are influenced by the mission profile metrics P_load and T_amb:

$$S_{N_f}(P_\mathrm{load}) = \frac{\partial N_f}{\partial P_\mathrm{load}} = \frac{\partial N_f}{\partial T_\mathrm{j}} \cdot \frac{\partial T_\mathrm{j}}{\partial P_\mathrm{load}} + \frac{\partial N_f}{\partial \Delta T_\mathrm{j}} \cdot \frac{\partial \Delta T_\mathrm{j}}{\partial P_\mathrm{load}} \tag{16a}$$

$$S_{N_f}(T_\mathrm{amb}) = \frac{\partial N_f}{\partial T_\mathrm{amb}} = \frac{\partial N_f}{\partial T_\mathrm{j}} \cdot \frac{\partial T_\mathrm{j}}{\partial T_\mathrm{amb}} + \frac{\partial N_f}{\partial \Delta T_\mathrm{j}} \cdot \frac{\partial \Delta T_\mathrm{j}}{\partial T_\mathrm{amb}}. \tag{16b}$$

In more general cases, if one denotes all studied mission profile metrics and relevant stress metrics as ξ_i and σ_j, respectively, then (16) can be summarized into

$$S_{N_f}(\xi_i) = \frac{\partial N_f}{\partial \xi_i} = \sum_j \frac{\partial N_f}{\partial \sigma_j} \cdot \frac{\partial \sigma_j}{\partial \xi_i} \tag{17}$$

where $\partial N_f/\partial \sigma_j$ and $\partial \sigma_j/\partial \xi_i$ correspond to the aforementioned definitions (14) and (8), respectively. Similar to (15), (17) can also be normalized as

$$S_{N_f}^{(\mathrm{n})}(\xi_i) = \frac{\partial N_f/N_f}{\partial \xi_i/\xi_i} = \sum_j \frac{\partial N_f}{\partial \sigma_j} \cdot \frac{\partial \sigma_j}{\partial \xi_i} \cdot \left(\frac{N_f}{\xi_i}\right)^{-1} \tag{18}$$

which denotes the percentage variation of N_f with regard to per-unit change of ξ_i.

Or alternatively, (17) can be written in the form of total differential for addressing the absolute variation of lifetime $\mathrm{d}N_f$ accounting for the change of all mission profile metrics

$$\mathrm{d}N_f = \sum_i \sum_j \frac{\partial N_f}{\partial \sigma_j} \cdot \frac{\partial \sigma_j}{\partial \xi_i} \cdot \mathrm{d}\xi_i. \tag{19}$$

Based on this, the lifetime sensitivity in relation to the mission profiles is calculated, as shown in Fig. 11, in percentage of N_f. The lifetime sensitivity reflects the overall influence of both mission profiles and the type of devices, including a balance of the different gradients in terms of ΔT_j and T_j according to (14a) and (14b), eventually inducing a nonmonotonic trend of variation. In contrast to Fig. 7, the results can be interpreted as follows.

1) The sensitivity is mapped to the sensing precision in the other way. If, e.g., a 1% error of lifetime estimation is acceptable when $\partial N_f/\partial T_\mathrm{amb} = -1.0\%/°\mathrm{C}$, then an approximation of 1°C sensing precision is sufficient.

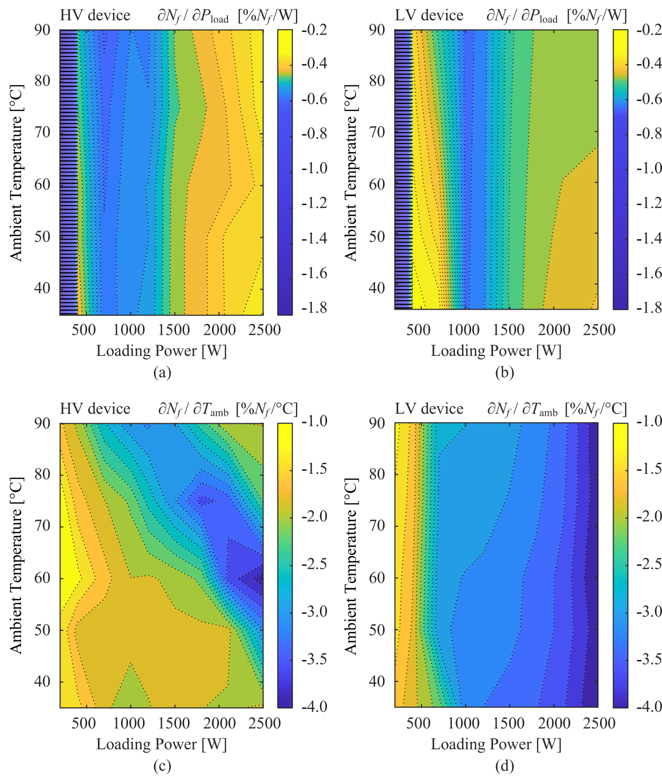

Fig. 11. Lifetime sensitivity of the studied devices in relation to the mission profile metrics T_amb and P_load: (a) and (c) for HV device, and (b) and (d) for LV device. The sensitivity metrics are labeled to the top of each subfigure individually.

2) When the lifetime is sensitive to the variation of mission profiles, there will be a larger variance of the estimated lifetime, which should also be noted, e.g., in reliability-oriented design and control, to ensure the robustness of the system models.
3) In terms of robustness, the error of measurement is a typical consideration. For example, it can be derived from (14) that the deviation of the sensitivity would be relevant to the relative rate of error in terms of the absolute measurement.

After all, more comprehensive validations of the sensitivity analysis require long-term tests under more varied mission profiles, which is not elaborated in this article due to the availability of lab facilities. In practice, it should also be noted that the sensitivity analysis for lifetime should act as comparative guidelines of reliability-oriented design approaches for power electronic systems, rather than fixed and explicit performance codes.

V. Extended Discussions

It is worth noting that the thermal impedance presented in Section II also features an uncertainty, which can result from manufacturing tolerances, measurement uncertainties, or modeling assumptions. We hereby extend the validations to lifetime sensitivity analysis on circuit parameter variations (equivalent transformer leakage inductance L_lk1 and output filter capacitance C_out), with simulated results presented in Table III. The average sensitivity is preliminarily exemplified, while a more accurate approach can be plotting the sensitivity alongside

TABLE III
NORMALIZED LIFETIME OF THE STUDY CASE AND SENSITIVITY ACCOUNTING FOR PARAMETER UNCERTAINTIES

L_{lk1}	0.5 μH	1.0 μH	1.5 μH	Average Sensitivity
HV	1.059	1.000	0.961	–0.098 [$\%N_\text{f}/\ \%L_{\text{lk1}}$]
LV	1.004	1.000	1.000	–0.004 [$\%N_\text{f}/\ \%L_{\text{lk1}}$]
C_{out}	2.75 μF	5.50 μF	8.25 μF	Average Sensitivity
HV	0.984	1.000	0.992	0.008 [$\%N_\text{f}/\ \%C_{\text{out}}$]
LV	0.989	1.000	1.003	0.014 [$\%N_\text{f}/\ \%C_{\text{out}}$]

Note: Estimated lifetime is normalized based on the rated condition.

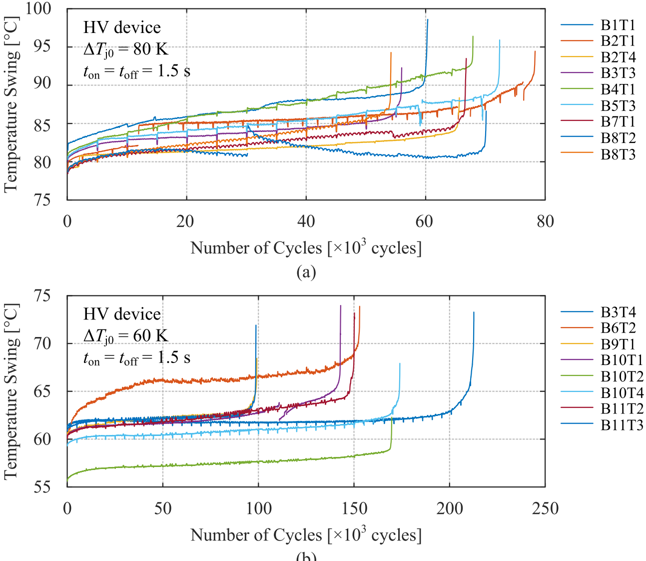

Fig. 12. Experimental results of power cycling tests of the studied power semiconductor devices for HV-side converter, under initial conditions: (a) $\Delta T_\text{j} = 80$ K and (b) $\Delta T_\text{j} = 60$ K, $t_\text{on} = t_\text{off} = 1.5$ s. The tests are conducted on several converter boards configured identically as specified in Fig. 8, HV boards, and B_xT_y denotes the group of test on the Converter Board x and Transistor y. The differences in junction temperature swings are demonstrated as time goes on, as a result of different R_{dson} increases related to device positions and manufacturing consistency.

different parameter values. In any case, different coupling of circuit components with the power devices is implied, which is a practical concern and worth being encompassed into more robust design of power electronic systems.

The scatter due to manufacturing tolerances is of particular importance for industrial applications, where the reliability must be ensured for a large number of manufactured devices. Fig. 12 preliminarily exhibits an example of the error in consistency due to the manufacturing of the devices. The differences of devices lead to varied lifetime obtained from power cycling tests, which should be described by statistical distributions. In principle, the most significant thermal impedance variations result from layers within the thermal path that have a high thermal resistance, e.g., thermal interfaces or electrical insulation with a low thermal conductivity. The thermal resistance of these layers is most sensitive to the thermal conductivity and to tolerances of the gap width or layer thickness, while additional variations may originate from voids inside the thermal interface material. Depending on the thermal coupling within the electronic component, losses of adjacent components may also influence the fit of a thermal impedance model. Typical sources for power loss variations can be electrical contact resistances or the drain–source resistance of transistors.

Similarly, the positions of devices on the PCBs may also lead to differences in thermal paths, including both the thermal paths to the ambient and the interdevice thermal coupling. It can also be seen from Fig. 12 the differences of devices within the same board and even the same arm of the converter. In hardware design, it is preferred to conduct thermal routing and align the power losses prior to implementation, to ensure prolonged overall system lifetime, where sensitivity analysis can be employed as an assistive tool.

To address this aspect, Monte Carlo simulations on the thermal performance, where probability distributions of geometrical tolerances and material properties are used, are one of the means to predict the overall uncertainty of a thermal resistance. In most cases, geometrical tolerances can be approximated with a Gaussian distribution while material properties or losses are bounded and require one-sided distributions, e.g., log-normal. There are multiple ways to obtain the probability distributions during the initial design phase. In case of electronic components, distributions or at least upper and lower bounds might be supplied by the manufacturers. The tolerances of geometrical dimensions are typically defined based on experience and later on ensured by process capability analysis during the industrialization. Additional effects, such as contact resistances or scattering in thermal conductivity of thermal interface materials, can be considered assuming upper and lower bounds. With this, the sensitivity of reliability can be handily evaluated as an effective reference for enhancing the liability of industrial manufacturing and reducing the unforeseen costs.

VI. CONCLUSION

This article has elaborated on the sensitivity analysis in reliability analysis for power electronic converters in order to address the need of small-signal analysis and provide proper interpretations therein. In this article, the sensitivity analysis is mathematically defined and explicated through two steps, highlighting the thermal stresses and lifetime models, respectively, and the influences of mission profiles are eventually portrayed. Case studies have also been rendered, which include both simulation and experimental testing results.

It can be concluded that sensitivity can not only guide the design and thermal monitoring of power electronic converters and systems but also act as an effective metric for encompassing robustness into reliability modeling and prediction. Therefore, potential future extension of this topic can be applications of this metric into practice, accounting for robustness in reliability modeling and control as well as stimulating effectiveness-optimized design of power electronic converters and systems.

ACKNOWLEDGMENT

The authors would acknowledge the technical support provided by the BMW Group, Munich, Germany.

REFERENCES

[1] D. Boroyevich, I. Cvetković, D. Dong, R. Burgos, F. Wang, and F. Lee, "Future electronic power distribution systems a contemplative view," in *Proc. 2010 12th Int. Conf. Optim. Elect. Electron. Equip.*, 2010, pp. 1369–1380.

[2] J. M. Carrasco et al., "Power-electronic systems for the grid integration of renewable energy sources: A survey," *IEEE Trans. Ind. Electron.*, vol. 53, no. 4, pp. 1002–1016, Jun. 2006.

[3] J. Biela, M. Schweizer, S. Waffler, and J. W. Kolar, "SiC versus Si—Evaluation of potentials for performance improvement of inverter and DC–DC converter systems by SiC power semiconductors," *IEEE Trans. Ind. Electron.*, vol. 58, no. 7, pp. 2872–2882, Jul. 2011.

[4] K. A. Kim, Y.-C. Liu, M.-C. Chen, and H.-J. Chiu, "Opening the box: Survey of high power density inverter techniques from the little box challenge," *CPSS Trans. Power Electron. Appl.*, vol. 2, no. 2, pp. 131–139, 2017.

[5] M. Hossain, N. Rahim, and J. a/l Selvaraj, "Recent progress and development on power DC-DC converter topology, control, design and applications: A review," *Renewable Sustain. Energy Rev.*, vol. 81, pp. 205–230, 2018.

[6] H. Wang and F. Blaabjerg, "Power electronics reliability: State of the art and outlook," *IEEE J. Emerg. Sel. Top. Power Electron.*, vol. 9, no. 6, pp. 6476–6493, Dec. 2021.

[7] Y. Song and B. Wang, "Survey on reliability of power electronic systems," *IEEE Trans. Power Electron.*, vol. 28, no. 1, pp. 591–604, Jan. 2013.

[8] H. Wang et al., "Transitioning to physics-of-failure as a reliability driver in power electronics," *IEEE J. Emerg. Sel. Top. Power Electron.*, vol. 2, no. 1, pp. 97–114, Mar. 2014.

[9] S. Rahimpour, H. Tarzamni, N. V. Kurdkandi, O. Husev, D. Vinnikov, and F. Tahami, "An overview of lifetime management of power electronic converters," *IEEE Access*, vol. 10, pp. 109688–109711, 2022.

[10] S. Yang, A. Bryant, P. Mawby, D. Xiang, L. Ran, and P. Tavner, "An industry-based survey of reliability in power electronic converters," *IEEE Trans. Ind. Appl.*, vol. 47, no. 3, pp. 1441–1451, May/Jun. 2011.

[11] H. Wang, K. Ma, and F. Blaabjerg, "Design for reliability of power electronic systems," in *Proc. IECON 2012-38th Annu. Conf. IEEE Ind. Electron. Soc.*, 2012, pp. 33–44.

[12] T. Dragičević, P. Wheeler, and F. Blaabjerg, "Artificial intelligence aided automated design for reliability of power electronic systems," *IEEE Trans. Power Electron.*, vol. 34, no. 8, pp. 7161–7171, Aug. 2019.

[13] J. V. M. Farias, A. F. Cupertino, V. d. N. Ferreira, H. A. Pereira, S. I. Seleme, and R. Teodorescu, "Reliability-oriented design of modular multilevel converters for medium-voltage STATCOM," *IEEE Trans. Ind. Electron.*, vol. 67, no. 8, pp. 6206–6214, Aug. 2020.

[14] J. Kuprat, C. H. van der Broeck, M. Andresen, S. Kalker, M. Liserre, and R. W. De Doncker, "Research on active thermal control: Actual status and future trends," *IEEE J. Emerg. Sel. Top. Power Electron.*, vol. 9, no. 6, pp. 6494–6506, Dec. 2021.

[15] M. Andresen, M. Liserre, and G. Buticchi, "Review of active thermal and lifetime control techniques for power electronic modules," in *Proc. 16th Eur. Conf. Power Electron. Appl.*, 2014, pp. 1–10.

[16] J. Falck, M. Andresen, and M. Liserre, "Active thermal control of IGBT power electronic converters," in *Proc. IECON - 41st Annu. Conf. IEEE Ind. Electron. Soc.*, 2015, pp. 1–6.

[17] D. Zhou, H. Wang, and F. Blaabjerg, "Mission profile based system-level reliability analysis of DC/DC converters for a backup power application," *IEEE Trans. Power Electron.*, vol. 33, no. 9, pp. 8030–8039, Sep. 2018.

[18] P. Kundur, *Power System Stability and Control*, 1st ed. New York, NY, USA: McGraw-Hill, 1994.

[19] J. He and X. Guan, "Uncertainty sensitivity analysis for reliability problems with parametric distributions," *IEEE Trans. Reliab.*, vol. 66, no. 3, pp. 712–721, Sep. 2017.

[20] R. Bayerer, T. Herrmann, T. Licht, J. Lutz, and M. Feller, "Model for power cycling lifetime of IGBT modules - various factors influencing lifetime," in *Proc. 5th Int. Conf. Integr. Power Electron. Syst.*, 2008, pp. 1–6.

[21] F. Hoffmann, N. Kaminski, and S. Schmitt, "Comparison of the power cycling performance of silicon and silicon carbide power devices in a baseplate less module package at different temperature swings," in *Proc. 33rd Int. Symp. Power Semicond. Devices ICs*, 2021, pp. 175–178.

[22] A. Birolini, *Reliability Engineering*, 8th ed. Berlin, Germany: Springer, 2017.

[23] X. Dong, A. Griffo, and J. Wang, "Multiparameter model order reduction for thermal modeling of power electronics," *IEEE Trans. Power Electron.*, vol. 35, no. 8, pp. 8550–8558, Aug. 2020.

[24] M. N. Touzelbaev, J. Miler, Y. Yang, G. Refai-Ahmed, and K. E. Goodson, "High-efficiency transient temperature calculations for applications in dynamic thermal management of electronic devices," *J. Electron. Packag.*, vol. 135, no. 3, 2013, Art. no. 031001.

[25] M. A. Miner, "Cumulative damage in fatigue," *J. Appl. Mech.*, vol. 12, no. 3, pp. A159–A164, 1945.

[26] H. Wang and F. Blaabjerg, "Reliability of capacitors for DC-link applications in power electronic converters—An overview," *IEEE Trans. Ind. Appl.*, vol. 50, no. 5, pp. 3569–3578, Sep./Oct. 2014.

Yubo Song (Member, IEEE) received the B.Sc. and M.Eng. degrees in electrical engineering from Shanghai Jiao Tong University, Shanghai, China, in 2016 and 2019, respectively, and the Ph.D. degree in energy technology from Aalborg University, Aalborg, Denmark, in 2023.

From May to July 2022, he was a Visiting Researcher with ELITE Grid Research Lab, University of Alberta, Edmonton, AB, Canada. He is currently a Postdoc with the Department of Energy, Aalborg University. His research interests include the control, stability, and reliability of power electronic systems and power electronic dominated grids.

Dr. Song was the recipient of the Spin-Outs Denmark grant in 2024.

Pascal A. Schirmer received the B.Eng. degree in electrical engineering from the University of Applied Sciences, Esslingen, Germany, in 2018, and the Ph.D. degree in electrical engineering from the University of Hertfordshire, Hatfield, U.K., in 2021.

Since 2021, he has been with R&D Department BMW AG, Munich, Germany, where he is responsible for the lifetime evaluation of power electronic systems. Furthermore, he is a Visiting Research Fellow with the University of Hertfordshire, where he focuses on NILM (software and hardware applications), and a Visiting Lecturer on electromobility with TAE, Esslingen.

Peter Schreivogel received the Dipl.-Ing. degree in aerospace engineering from Technical University Dresden, Dresden, Germany, in 2009, the Research master's degree in fluid dynamics from the Von Karman Institute for Fluid Dynamics, Rhode-Saint-Genèse, Belgium, in 2011, and the Ph.D. degree in aerospace engineering from the University of the Federal Armed Forces Munich, Munich, Germany, in 2015.

From 2015 to 2018, he was a thermo-fluid systems Engineer with Rolls-Royce Deutschland. Since 2018, he has been a Specialist in thermal management of power electronics with BMW AG, Munich. His research interests include advanced cooling technologies, such as pulsating heat pipes and reduced order thermal modeling.

Dr. Schreivogel was the recipient of the DLR technology award in 2009 and the Claudius Dornier Jr. dissertation award in 2016.

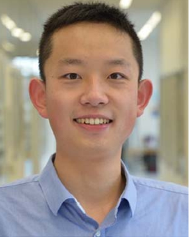

Kaichen Zhang (Member, IEEE) received the B.Eng. degree in electrical engineering and automation from the Huazhong University of Science and Technology, Wuhan, China, in 2018, and the M.S. degree in energy technology (power electronics and drives) in 2020 from Aalborg University, Aalborg, Denmark, where he is currently working toward the Ph.D. degree in energy technology.

From September 2019 to February 2020, he was with ABB Corporate Research Center, Baden-Dättwil, Switzerland. His research focuses on the reliability of power electronic components.

Huai Wang (Senior Member, IEEE) received the B.E. degree in electrical engineering from the Huazhong University of Science and Technology, Wuhan, China, in 2007, and the Ph.D. degree in power electronics from the City University of Hong Kong, Hong Kong, in 2012.

From August to September 2014, he was a Visiting Scientist with ETH Zurich, Zurich, Switzerland, and from September to November 2013, he was with the Massachusetts Institute of Technology, Cambridge, MA, USA. In 2009, he was with the ABB Corporate Research Center, Baden, Switzerland. He is currently a Professor with AAU Energy, Aalborg University, Aalborg, Denmark, where he leads the group of Reliability of Power Electronic Converters (ReliaPEC) and the mission on digital transformation and AI. His research interests include the fundamental challenges in modeling and validating power electronic component failure mechanisms and application issues in system-level predictability, condition monitoring, circuit architecture, and robustness design.

Dr. Wang was the recipient of the Richard M. Bass Outstanding Young Power Electronics Engineer Award from the IEEE Power Electronics Society in 2016 and the 1st Prize Paper Award from IEEE TRANSACTIONS ON POWER ELECTRONICS in 2021. He is currently an Associate Editor of IEEE JOURNAL OF EMERGING AND SELECTED TOPICS IN POWER ELECTRONICS and IEEE TRANSACTIONS ON POWER ELECTRONICS. He was elected as a Member of the Danish Academy of Technical Sciences in 2023.

Frede Blaabjerg (Fellow, IEEE) received the Ph.D. degree in electrical engineering from Aalborg University, Aalborg, Denmark, in 1995.

From 1987 to 1988, he was with ABB-Scandia, Randers, Denmark. He became an Assistant Professor in 1992, an Associate Professor in 1996, and a Full Professor of power electronics and drives in 1998. In 2017, he became a Villum Investigator. He is *honoris causa* with University Politehnica Timisoara, Timisoara, Romania, and Tallinn Technical University, Tallinn, Estonia. He has authored or coauthored more than 600 journal papers in the fields of power electronics and its applications. He is the coauthor of four monographs and editor of ten books in power electronics and its applications. His current research interests include power electronics and its applications, such as in wind turbines, PV systems, reliability, harmonics, and adjustable speed drives.

Dr. Blaabjerg was the recipient of the 32 IEEE Prize Paper Awards, the IEEE PELS Distinguished Service Award in 2009, the EPE-PEMC Council Award in 2010, the IEEE William E. Newell Power Electronics Award 2014, the Villum Kann Rasmussen Research Award 2014, the Global Energy uPrize in 2019, and the 2020 IEEE Edison Medal. He was the Editor-in-Chief of IEEE TRANSACTIONS ON POWER ELECTRONICS from 2006 to 2012. He has been a Distinguished Lecturer for the IEEE Power Electronics Society from 2005 to 2007 and for the IEEE Industry Applications Society from 2010 to 2011 as well as 2017 to 2018. During 2019–2020, he was the President of the IEEE Power Electronics Society. He is the Vice-President of the Danish Academy of Technical Sciences too. He was nominated in 2014–2019 by Thomson Reuters to be among the 250 most cited researchers in engineering in the world.